



Finite Element Investigation of Fracture Risk Under Postero-Anterior Mobilization on a Lumbar Bone in Elderly With and Without Osteoporosis

Chadapa Rungruangbaiyok¹ · Fahimeh Azari² · G. Harry van Lenthe² · Jos Vander Sloten² · Boonsin Tangtrakulwanich³ · Surapong Chatpun^{1,4}

Received: 27 October 2020 / Accepted: 19 March 2021 / Published online: 15 April 2021
© Taiwanese Society of Biomedical Engineering 2021

Abstract

Purpose Postero-anterior (PA) mobilization is widely used to manage low back pain by physiotherapists. The PA load is applied through the spinous process of a vertebra. Low bone density is a counter-indication of PA mobilization, whether PA mobilization may cause fractures in fragile vertebrae is unclear. Therefore, the aim of this study was to quantify the role of bone density on a fracture risk in the first lumbar vertebra subjected to PA load.

Methods A finite element model of the first lumbar (L1) vertebra of an elderly female was created to predict the fracture risk of the PA mobilization. The von Mises stress and minimum principal strain were used as the assessment indicators. Three different bone density cases were evaluated to reflect healthy, osteoporotic, and severe osteoporotic conditions by assuming heterogeneous moduli based on local bone density converted from computed tomographic images.

Results In the severe osteoporotic condition under PA load, the maximum von Mises stress and largest compressive strain occurred in the pedicles and spinous process. These stress and strain exceeded the yield stress and yield strain indicating a high risk for failure. The resulted stress and strain were also excessive in the pedicles for healthy and moderate osteoporotic conditions.

Conclusions PA mobilization can increase the risk of vertebra fracture in elderly with osteoporosis. The pedicles and spinous process of osteoporotic L1 vertebra are the critical regions prone to fracture. We recommend that it is crucial to be reduce force when applying the PA mobilization to elderly with osteoporosis.

Keywords Postero-anterior mobilization · Osteoporosis · Finite element analysis · Minimum principal strain

1 Introduction

Postero-anterior (PA) mobilization is a manual physical therapy technique which is a passive movement with low speed. It can be divided into a passive oscillatory movement and a sustained stretching [1]. PA mobilization can be applied to assess and treat the impairments of the human spine by applying a force on a spinous process. The effects of PA mobilization are pain relief, reducing spinal stiffness and increasing range of motion of the spine [2–4]. It is shown that the PA mobilization can produce a physiological movement in the sagittal plane. Specifically, PA loads generate a three-point bending or passive physiological back extension [5–7]. Furthermore, PA loads demonstrated the anterior displacement of a spinous process [5]. The application of PA mobilization induces stresses inside the bone tissue, which could potentially lead to failure when the bone is weak, such

✉ Surapong Chatpun
surapong.c@psu.ac.th

¹ Faculty of Medicine, Department of Biomedical Sciences and Biomedical Engineering, Prince of Songkla University, Songkhla 90110, Thailand
² Faculty of Engineering Science, Department of Mechanical Engineering, KU Leuven, Biomechanics section, Leuven, Belgium
³ Faculty of Medicine, Department of Orthopedics, Prince of Songkla University, Songkhla 90110, Thailand
⁴ Faculty of Medicine, Institute of Biomedical Engineering, Prince of Songkla University, Songkhla 90110, Thailand

as in patients with osteoporosis, a bone disease occurring in elderly and which is characterized low bone density, leading to bone fragility and susceptibility to fracture. Consequently, osteoporosis is a contraindication for spinal mobilization [1]. In East Asia, osteoporosis seems to be under-diagnosed and under-treated [8].

Up to now, there is no empirical evidence that reports a relationship between the PA mobilization and the incidence of spine fracture. Several *in vitro* studies investigated the fracture risk produced by PA load [9–11]. These studies found that the failure load of cadaveric thoracic vertebrae was higher than the load that was applied *in vivo* by a physiotherapist [11]. These studies also demonstrated that the fracture site caused by PA load was the spinous process of the thoracic spine. These could be at risk, especially when in case of low bone quality, which warrants further investigation into the safety using of PA mobilization on lumbar spine. In addition, low back pain is the most common back pain, and therefore, PA mobilization would preferentially be applied to the lumbar spine. Accordingly, the fracture risk investigation of lumbar vertebra under the PA load is crucial. However, there was no study to investigate the safety of using PA mobilization on lumbar osteoporotic bone yet both *in vivo* and *in vitro* studies. Therefore, *in silico* study using the finite element analysis (FEA), which is an engineering analysis technique, has been introduced to clinical decision making, especially in orthopedics [12–14], can also provide the accuracy prediction. FEA has been used in osteoporosis study due to the complex structure of bones in several objectives such as predicting the bone stiffness, fracture site [15, 16]. Moreover, FEA provided the information of the effect of mechanical stimuli in osteoporotic bone [17].

The FEA study revealed that 100 N of PA mobilization possibly produces a crack initiation at lumbar vertebra with osteoporotic condition at laminae and pedicles [18]. However, that study investigated the effect of PA mobilization on male elderly L1 vertebra using homogeneous bone mechanical properties. Several studies have shown that heterogeneity of bone plays an important role in fracture analysis [12, 13, 16, 19, 20]. Furthermore, the prevalence of fracture related to osteoporosis in menopausal female was higher than elderly male [21]. Additionally, the shape of the female and male lumbar vertebral bone was different significantly in size [22]. Hence, the fracture risk prediction in case of PA mobilization will be more accurate if the bone properties are closer to reality by assigning heterogeneous bone properties and the prediction is performed on elderly female lumbar vertebra. As to our knowledge, there are no studies using heterogeneity of bone properties for female osteoporotic bone from HU value of computer tomography (CT) images in the FEA study. Therefore, this study aimed to quantify the role of bone density on a fracture risk in the L1 vertebra subjected to PA mobilization.

2 Materials and Methods

2.1 Finite Element Modelling

The L1 vertebra geometry was segmented and reconstructed from CT images (Fig. 1), obtained by means of Toshiba Aquilion Prime, of a non-osteoporotic 60-year-old female. The slice thickness of CT images was 1 mm. Image segmentation and three dimensional geometry reconstruction were performed using Mimics v20 (Materialise Inc., Leuven, Belgium). Upper and lower polymethylmethacrylate (PMMA) plates were designed and assembled with L1 vertebra in order to reflect intervertebral disc spaces using the Materialise 3-matic v12 module in the Mimics software. A volume mesh was also performed using the Materialise 3-matic v12 module. Then the model was exported to the commercial finite element software ABAQUS 2019 (Dassault Systemes, Vélizy-Villacoublay, France) to perform a finite element analysis. A mesh sensitivity study was employed to confirm the appropriateness of this finite element mesh. Specifically, a mesh refinement study was performed, evaluating meshes with 7,373 to 58,728 elements. The mesh convergence check was also performed with the difference in von Mises stress at center of mid-transverse section of L1 vertebra less than 1.5%. The L1 vertebra with PMMA plates was thus represented by a finite element model consisting of 29,364 tetrahedral elements. The geometry of the L1 vertebra model was validated with published human cadaveric studies using quantitative anatomy of lumbar [23, 24]. This project was approved by the ethical committee, faculty of medicine, Prince of Songkla University (REC.61–364-25–2).

Material properties are shown in Table 1. The heterogeneous modulus distribution was based on a density-elasticity relationship obtained from CT images [25]. Morgan et al. showed that the bone's apparent density ρ (g/cm^3) calculated from the Hounsfield Units (HU) can be used to estimate Young's modulus (E ; MPa) as follows:

$$\rho = 0.0556 + 0.001244HU \quad (1)$$

$$E = 4730\rho^{1.56} \quad (2)$$

The Young's modulus was assigned on element by element basis and it depended on the local bone density. For the healthy case, the Young's modulus varied between 0.56 MPa and 10.71 GPa. The distribution of Young's modulus in mid-transverse and mid-sagittal sections of L1 vertebra is shown in Fig. 2. We then mimicked the osteoporotic bone conditions by decreasing Young's modulus in each region by 25% for an osteoporotic bone and 50% for a severe osteoporotic bone (as shown in Table 1).

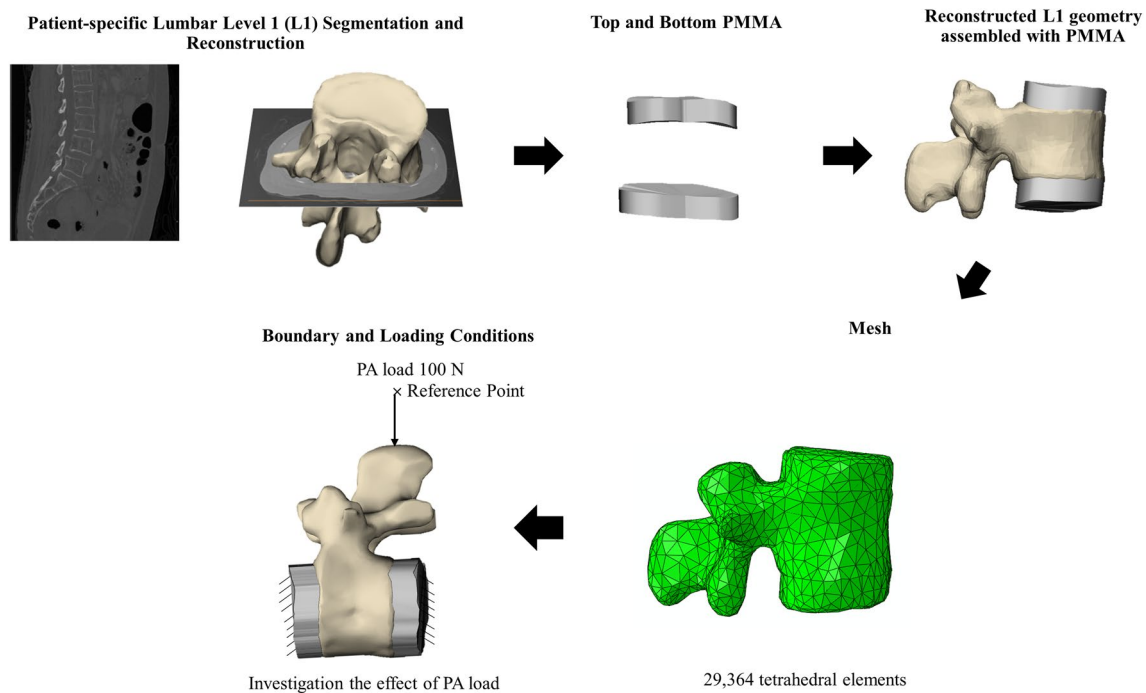


Fig. 1 Steps of building a L1 vertebra with PMMA plates models and the boundary conditions for the corroboration test and the PA load investigation

Table 1 Material properties assigned to the L1 vertebra model

Model	Young's modulus (E, MPa)	Poisson's ratio (ν)
L1 vertebra		
Healthy	0.56 – 10,706.5	$\left\{ \begin{array}{l} 0.2 \text{ *}, \text{ if } E < 1,000 \\ 0.3 \text{ *}, \text{ if } E \geq 1,000 \end{array} \right.$
Osteoporotic		
Severe osteoporotic		
PMMA plate	2,500	0.3

*refer to Poisson's ratio obtained from Goel's study[39]

2.2 Boundary and Loading Conditions

The condition in this study mimicked the loading condition during PA mobilization. The bottom surface of the lower PMMA plate and the top surface of the upper PMMA plate were fixed in all directions. The posterior surface of the spinous process was coupled with a reference point behind the spinous process. A 100 N force was applied on the reference point along the Y-axis to simulate the postero-anterior force from the physiotherapist as shown in Fig. 1. Four positions in the mid-transverse section of L1 vertebra were compared i.e. center, pedicles, laminae, and spinous process.

2.3 Post-Processing Analysis

Numerical results obtained via FEA were post-processed for fracture risk assessment. In general, the von Mises stress measure is widely used in the FE studies for analyzing load-transfer mechanisms and failure material behavior. In some cases, von Mises stress does not provide effective indications in term of fracture risk in materials such bone. Therefore, other indications were introduced to evaluate the fracture risk level such as minimum principal strain. In our study, fracture risk level was evaluated by comparing the von Mises stress and the minimum principal strain to the yield stress and the yield strain, respectively (Table 2). The mean

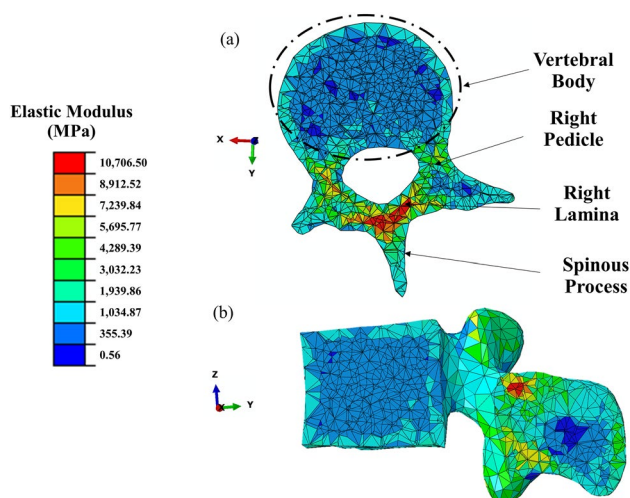


Fig. 2 Young's moduli in **a** a mid-transverse section and **b** a mid-sagittal section of L1 vertebra (healthy model)

Table 2 Yield stress and yield strain of lumbar vertebral bone

L1 Structures	Yield stress (MPa)	Yield strain (micro-strain)
Vertebral body	2.66 ^a	-10,000 ^c
Pedicles	13.13 ^b	-10,000 ^c
Laminae	13.13 ^b	-10,000 ^c
Spinous process	2.11 ^b	-10,000 ^c

^a and ^b refer to the yield stress obtained from Li's study and Kurutz's study, respectively. [29, 30] and ^c refers to the yield strain of trabecular bone modified from Røhl's study.[32]

von Mises stress and the maximum magnitude of minimum principal strain of four structures of the L1 vertebra (vertebral body, pedicles, laminae, and spinous process) were reported.

3 Results

As the quantitative anatomy of lumbar, the L1 vertebra model in various linear dimensions; vertebral body lateral width, vertebral body anterior–posterior (AP) depth, vertebral body height, transverse process width, spinal canal width and depth, pedicle width and height both sides, and spinous process length, were compared to the published experimental data [23, 24]. The reasonable agreement was found as shown in Fig. 3b.

Under the 100 N postero-anterior load, while the stresses were rather similar for the healthy, osteoporotic, and severe osteoporotic cases, the strains were much higher for the latter case (Figs. 4, 5). The posterior structures of L1 vertebra,

which consisted of pedicles, laminae, and spinous process, demonstrated higher von Mises stresses and larger magnitude of minimum principal strains than the vertebral body.

While the Young's modulus differed substantially between the three bone models, the von Mises stress distribution did not differ markedly (< 10 percent). The distribution of the magnitude of minimum principal strains tended to increase when the Young's modulus was reduced, and it was more predominant to the minimum principal strain than the von Mises stress.

Mean, standard deviation and maximum magnitude of von Mises stress and minimum principal strain are shown in Tables 3 and 4, respectively. For all bone conditions, the maxima occurred at the nearly mid-transverse position of right pedicle. When the yield stress criterion was taken into account (as shown in Table 2), the structures where the maximum von Mises stress exceeded the yield stress criterion were spinous process, vertebral body and pedicles (all models). According to the yield strain criterion (as shown in Table 2), the structures where the maximum magnitude of the minimum principal strain exceeded the yield strain criterion were pedicles (osteoporotic and severe osteoporotic model) and spinous process (only severe osteoporotic model).

4 Discussion

This study showed that postero-anterior mobilization in elderly female osteoporotic lumbar vertebral bone can cause fracture of the pedicles and spinous process of lumbar vertebra. Furthermore, the comparison of contour plot between Young's modulus and both stresses and strains (as shown in Figs. 4, 5) emphasized that the minimum principal strain reflected the dominant difference among different bone densities better than the von Mises stress when the lumbar vertebra is under postero-anterior mobilization. The comparison also showed that the lower moduli area induced the higher strains especially on the spinous process (Fig. 5). Meanwhile, the stress was not altered by the variation of Young's moduli (Fig. 4).

We validated our FE model by comparing linear dimensions of L1 vertebra geometry with the experimental studies [23, 24] as shown in Fig. 3. Several FEA studies suggested to validate the geometry parameters prior perform simulation because the resolution of CT scan affected the accuracy of the geometry [26, 27]. We did not use the high resolution of CT scan, therefore the accuracy of L1 vertebra dimensions can be altered during the reconstruction process. However, after the geometry validation study, we found the reasonable agreement of L1 vertebra geometry parameters between the present FE model with experimental studies.

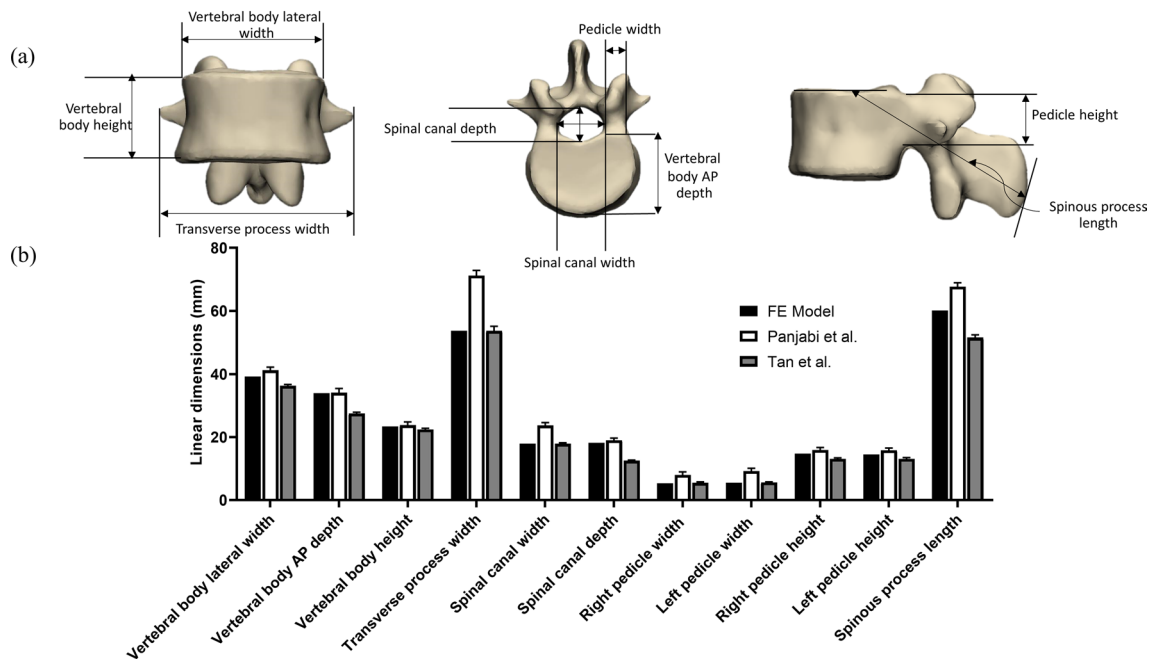


Fig. 3 **a** The illustration of the various dimensions of L1 vertebra and **b** a comparison between the L1 vertebra geometry dimensions of the present FE model and human cadaveric studies

Upon application of 100 N of postero-anterior force, the distribution of von Mises stress and minimum principal strain demonstrated that the posterior side of L1 vertebra was loaded more than the body of L1 vertebra, especially on the pedicle. This can be explained by the application of the force to the spinous process which is connected to the vertebral body via the pedicles. As the geometry of the pedicles resembles a thin bridge structure, the bending consequently occurs at the pedicles and the spinous process which are moved downward and anteriorly. Physiotherapists can feel the displacement of the spinous process when they perform the PA mobilization. This phenomenon is confirmed by an *in vivo* study [5]. They found that the spinous process displaced anteriorly due to the PA mobilization. When the spinous process was moved anteriorly, the pedicles were experiencing more bending. Therefore, pedicles are a critical structure due to the PA load. The previous work we showed that the laminae and pedicles of elderly male lumbar vertebra were susceptible to fracture under the PA load [18]. Furthermore, our prediction also showed that, in a severe osteoporosis case, not only the pedicles but also spinous process of the L1 vertebra was a high-risk fracture site. According to the contour plot of Young's modulus of L1 in the current study (Fig. 2), the spinous process demonstrated low elastic moduli. Therefore, the heterogeneous properties assignment in FEA can lead to different outcomes. For the spinous process failure prediction, a previous study of the failure characteristic of the thoracic spine under the PA load revealed

that the failure site occurred at the spinous process in healthy bone conditions [11], but our prediction demonstrated that the spinous process can be a failure site in a severe osteoporosis case only. The possible reason for different findings is based on the different width of the spinous process between thoracic and lumbar spines. The width of thoracic spinous processes is less than the width of lumbar spinous processes. Consequently, the thoracic spinous process is subjected to higher stress than the lumbar spinous process for the same loading. However, the PA load which can cause a fracture in the healthy bone conditions in the experimental study was higher than the one applied in the current study. Therefore, it is relevant to assigned bone mechanical properties close to reality to achieve higher accuracy.

For the fracture risk, the von Mises stress and minimum principal strain have been widely used as the indicators [12–14, 19, 28]. In this study, the yield stress of each part of the lumbar vertebra was adopted from previous study [29]. However, the yield stress for the pedicle was lack. There was only one biomechanical study of the ultimate stress of the posterior part of the adult cadaveric lumbar vertebra [29]. It reported the ultimate stress of the laminae and spinous process. Therefore, we extrapolated the ultimate stress of the pedicle same as the ultimate stress of the laminae based on the similar range of elastic moduli to be a yield stress of pedicle in our study. According to the previous computational studies, the yield criterion of strain was set at -10,000 microstrain [30, 31]. Furthermore, the

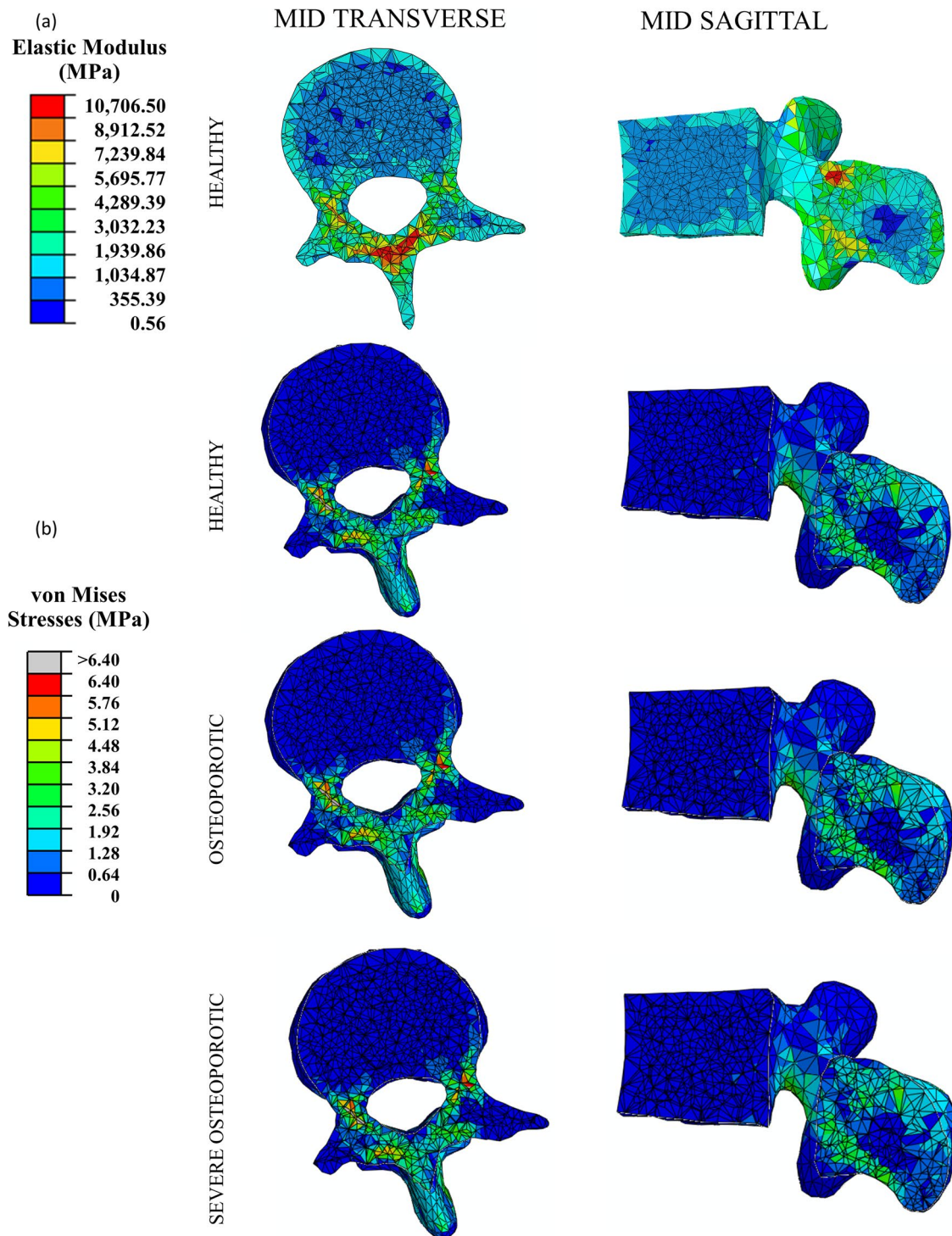


Fig.4 **a** Contour plot of Young's moduli in a mid-transverse section and a mid-sagittal section of L1 vertebra. **b** Contour plot of von Mises stresses in mid-transverse section and mid-sagittal section of deformed L1 vertebra under 100 N postero-anterior load

previous experimental study demonstrated the ultimate strain for trabecular bone under the compression ranged from $-3,000$ to $-27,900$ microstrain (with an average of $-11,000$ microstrain) [32]. In our study, the fracture risk

occurred at the pedicles of moderate and severe osteoporotic L1 vertebra and in the spinous process of severe osteoporotic L1 vertebra where lower elastic modulus presented.

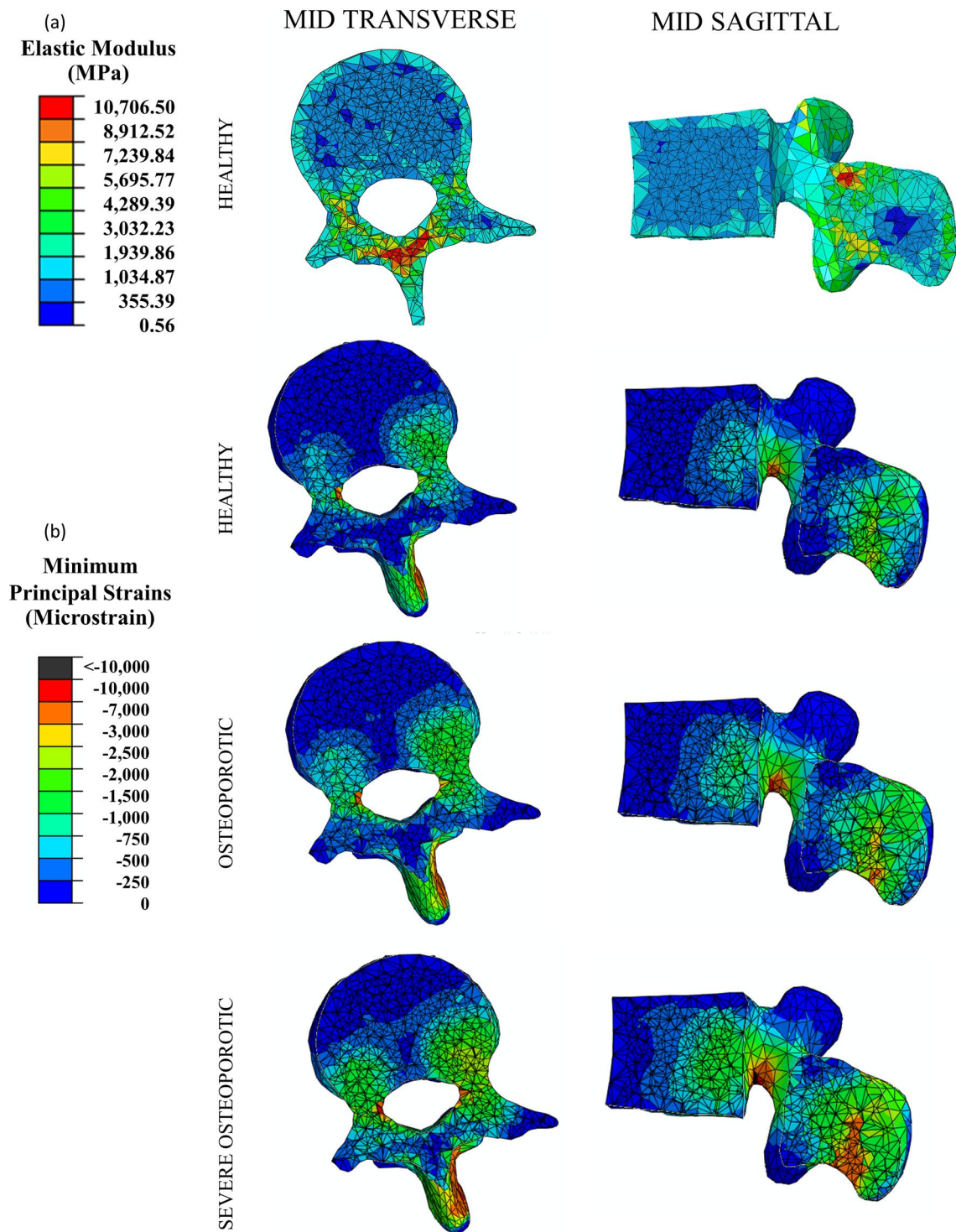


Fig.5 **a** Contour plot of Young’s moduli in a mid-transverse section and a mid-sagittal section of L1 vertebra. **b** Contour plot of minimum principal strain in mid-transverse section and mid-sagittal section of deformed L1 vertebra under 100 N postero-anterior load

Our osteoporotic bone FE models demonstrated higher magnitude of minimum principal strain distribution in the L1 vertebra compared to the healthy bone. It emphasizes

that osteoporotic bone is more susceptible to fracture. The spine is one of the most common osteoporotic fracture sites [33], particularly in the mid- thoracic and thoracolumbar

Table 3 Mean and maximum (Max.) of von Mises stresses of L1 vertebra under 100 N postero-anterior load

Structures		Healthy	Osteoporotic	Severe Osteoporotic
Vertebral Body	Mean (SD)	0.16(0.24)	0.16(0.24)	0.15(0.24)
	Max. magnitude	4.07	4.07	4.07
	Max. point	Right conjunction between body and pedicle		
Pedicles	Mean (SD)	1.60(1.85)	1.60(1.85)	1.60(1.85)
	Max. magnitude	19.25	19.22	19.18
	Max. point	Nearly mid-transverse position of right pedicle		
Laminae	Mean (SD)	2.10(1.72)	2.10(1.72)	2.10(1.72)
	Max. magnitude	12.18	12.17	12.16
	Max. Point	Right lamina		
Spinous process	Mean (SD)	1.44(1.33)	1.44(1.33)	1.44(1.33)
	Max. magnitude	12.36	12.36	12.36
	Max. point	Right lower edge		

von Mises stress's unit is in MPa

Table 4 Mean and maximum (Max.) magnitude of minimum principal strains of L1 vertebra under 100 N postero-anterior load

Structures		Healthy	Osteoporotic	Severe Osteoporotic
Vertebral Body	Mean (SD)	-280(269)	-370(357)	-540(532)
	Max. magnitude	-1,520	-2,023	-3,031
	Max. point	Right conjunction between body and pedicle		
Pedicles	Mean (SD)	-669(836)	-890(1,113)	-1,330(1,666)
	Max. magnitude	-7,733	-10,282	-15,374
	Max. point	Nearly mid-transverse position of right pedicle		
Laminae	Mean (SD)	-433(329)	-577(438)	-865(656)
	Max. magnitude	-4,196	-5,578	-8,361
	Max. point	Right lamina		
Spinous process	Mean (SD)	-992(1,020)	-1,323(1,359)	-1,984(2,039)
	Max. magnitude	-6,657	-8,876	-13,313
	Max. point	Right lower edge		

minimum principal strain's unit is in microstrain

regions [34, 35], which is T10-L2 vertebrae. Since the pattern of osteoporotic fractures in the vertebra rather reflect a non-traumatic fracture, activities of daily living might cause fractures. A previous FEA study [36] demonstrated that activities producing flexion moment to the thoracolumbar region such as trunk forward bending might cause osteoporotic fractures. However, the PA mobilization produces an extension moment to the spine [5–7], which is an antagonist action with the trunk flexion. In addition, the non-traumatic fracture in posterior bony column of lumbar spine is rarely found [37, 38]. Therefore, 100 N of PA mobilization in our study may not cause a severe fracture in the posterior bony column, but it can cause mild fracture especially at the pedicles and spinous process. In an experimental study of the effect of PA mobilization on the thoracic vertebrae [11], the authors also revealed the spinous process as the fracture site.

Our analysis of the variation of the bone properties demonstrated that only the minimum principal strain reflected the difference among bone properties obviously. Based on

the simple equation of stress, stress depends on the geometry and the load application. However, stress would be altered when the material reaches the plastic phase because the material is deformed. The heterogeneity of the material also affects the stress distribution. Furthermore, when the heterogeneous property was considered, notable changes in results are observed. Therefore, the conversion of CT image information (Hounsfield number) of bone to the corresponding bone property (Young's modulus) is important as the reliability of the simulation results depends on bone property, especially in the case of osteoporotic bones.

Our L1 vertebra finite element model had several limitations. Firstly, we did not validate our FEM with in vitro mechanical testing, but we corroborated it with the published literature results [20] (see the supplement). Secondly, we did not include muscle force in our model, because we focused only on static PA load which is a passive load. In clinical practice, the PA mobilization can be used as a static force to investigate the tension of the spine structure. Furthermore,

the repetitive load of PA mobilization, which is the dynamic force, can be used for a treatment session. Therefore, the effect of PA dynamic load on osteoporotic heterogeneous vertebrae should be further investigated. In addition, the effects on the adjacent vertebrae subjected to the PA load indirectly should be further studied.

5 Conclusion

This study performed the CT images based finite element analysis to investigate the effect of PA mobilization on the heterogeneous L1 vertebra model of elderly female. It revealed that PA mobilization can increase the risk of vertebra fracture in elderly female with osteoporosis. The critical points were the pedicles and the spinous process of osteoporotic L1 vertebra. We would like to emphasize that when PA mobilization is applied on elderly with osteoporosis, it should be performed carefully since it may cause a lumbar spine fracture.

Acknowledgements We would like to gratefully acknowledge the PhD scholarship by Walailak University and an international research internship scholarship by Faculty of Medicine, Prince of Songkla University awarded to Mrs. Chadapa Rungruangbaiyok. We would like to thank Biomechanics Section, KU Leuven University for the research internship hosting. We also thank Dr. Atichart Kwanyuang for great advices about the computational simulation. We appreciate the very kind support and suggestions from CERLab members.

Declarations

Conflict of interest The authors declare that they have no conflict of interest.

Ethical Approval This project was approved by the ethical committee, faculty of medicine, Prince of Songkla University (REC.61–364-25–2).

Informed consent This article does not contain any studies with human participants or animals performed by any of the authors.

References

- Maitland, G. D. (2005). *Maitland's Vertebral Manipulation*. . Oxford: Elsevier Butterworth-Heinemann.
- Shah, S. G., & Kage, V. (2016). Effect of seven sessions of posterior-to-anterior spinal mobilisation versus prone press-ups in non-specific low back pain-randomized clinical trial. *Journal of Clinical and Diagnostic Research*, *10*(3), 10–13.
- Kamel, D. M., Raoof, N. A. A., & Tantawy, S. A. (2016). Efficacy of lumbar mobilization on postpartum low back pain in Egyptian females: A randomized control trial. *Journal of Back and Musculoskeletal Rehabilitation*, *29*(1), 55–63.
- Kanlayanaphotporn, R., Chiradejnant, A., & Vachalathiti, R. (2010). Immediate effects of the central posteroanterior mobilization technique on pain and range of motion in patients with mechanical neck pain. *Disability and Rehabilitation*, *32*(8), 622–628.
- Lee, R., & Evans, J. (1997). An in vivo study of the IV movements produced by PA mobilization. *Clinical Biomechanics*, *12*(6), 400–408.
- Powers, C. M., Kulig, K., Harrison, J., & Bergman, G. (2003). Segmental mobility of the lumbar spine during a posterior to anterior mobilization: Assessment using dynamic MRI. *Clinical Biomechanics*, *18*(1), 80–83.
- Kulig, K., Landel, R., & Powers, C. M. (2004). Assessment of Lumbar Spine Kinematics Using Dynamic MRI: A Proposed Mechanism of Sagittal Plane Motion Induced by Manual Posterior-to-Anterior Mobilization. *Journal of Orthopaedic and Sports Physical Therapy*, *34*(2), 57–64.
- Cheung, E. Y. N., Tan, K. C. B., Cheung, C.-L., & Kung, A. W. C. (2016). Osteoporosis in East Asia: Current issues in assessment and management. *Osteoporosis and Sarcopenia*, *2*(3), 118–133.
- Moro, M., Hecker, A. T., Boussein, M. L., & Myers, E. R. (1995). Failure load of thoracic vertebrae correlates with lumbar bone mineral density measured by DXA. *Calcified Tissue International*, *56*(3), 206–209.
- Bürklein, D., Lochmüller, E. M., Kuhn, V., Grimm, J., Barkmann, R., Müller, R., & Eckstein, F. (2001). Correlation of thoracic and lumbar vertebral failure loads with in situ vs. ex situ dual energy X-ray absorptiometry. *Journal of Biomechanics*, *34*(5), 579–587.
- Sran, M. M., Khan, K. M., Zhu, Q., McKay, H. A., & Oxland, T. R. (2004). Failure characteristics of the thoracic spine with a posteroanterior load: Investigating the safety of spinal mobilization. *Spine*, *29*(21), 2382–2388.
- Bessho, M., & A. I. O., Matsuyama, J., Matsumoto, T., & Imai, K. (2007). Prediction of strength and strain of the proximal femur by a CT-based finite element method. *Journal of Biomechanics*, *40*, 1745–1753.
- Schileo, E., Taddei, F., Cristofolini, L., & Viceconti, M. (2008). Subject-specific finite element models implementing a maximum principal strain criterion.pdf. *Journal of Biomechanics*, *41*, 356–367.
- Tanck, E., Van Aken, J. B., Van Der Linden, Y. M., Schreuder, H. W. B., Binkowski, M., Huizenga, H., & Verdonchot, N. (2009). Pathological fracture prediction in patients with metastatic lesions can be improved with quantitative computed tomography based computer models. *Bone*, *45*(4), 777–783.
- Klintström, E., Klintström, B., Moreno, R., Brismar, T. B., Pahr, D. H., & Smedby, Ö. (2016). Predicting trabecular bone stiffness from clinical cone-beam CT and HR-pQCT Data; an In vitro study using finite element analysis. *PLoS ONE*, *11*(8), 1–19.
- Giambini, H., Qin, X., Dragomir-Daescu, D., An, K. N., & Nassr, A. (2016). Specimen-specific vertebral fracture modeling: a feasibility study using the extended finite element method. *Medical and Biological Engineering and Computing*, *54*(4), 583–593.
- Sandino, C., McErlain, D. D., Schipilow, J., & Boyd, S. K. (2017). Mechanical stimuli of trabecular bone in osteoporosis: A numerical simulation by finite element analysis of microarchitecture. *Journal of the Mechanical Behavior of Biomedical Materials*, *66*, 19–27.
- Boonyoung, C., Kwanyuang, A., & Chatpun, S. (2019). A finite element study of posteroanterior lumbar mobilization on elderly vertebra geometry. In BMEiCON 2018 - 11th Biomedical Engineering International Conference (pp. 1–4).
- Imai, K., Ohnishi, I., & Bessho, M. (2006). Nonlinear Finite Element Model Predicts Vertebral Bone Strength and Fracture Site. *Spine*, *31*(16), 1789–1794.
- Erdem, I., Truumees, E., & van der Meulen, M. C. H. (2013). Simulation of the behaviour of the L1 vertebra for different material properties and loading conditions. *Computer Methods in Biomechanics and Biomedical Engineering*, *16*(7), 736–746.

21. Ji, M. X., & Yu, Q. (2015). Primary osteoporosis in postmenopausal women. *Chronic Diseases and Translational Medicine*, 1(1), 9–13.
22. Gilsanz, V., Boechat, M. I., Gilsanz, R., Loro, M. L., Roe, T. F., & Goodman, W. G. (1994). Gender differences in vertebral sizes in adults: Biomechanical implications. *Radiology*, 190(3), 678–682.
23. Panjabi, M. M., Vijay, G., Oxland, T. R., Koichiro, T., Joanne, D., Martin, K., & Mark, P. (1992). Human lumbar vertebrae quantitative three-dimensional anatomy. *Spine*, 17, 299–306.
24. Tan, S. H., Teo, E. C., & Chua, H. C. (2004). Quantitative three-dimensional anatomy of cervical, thoracic and lumbar vertebrae of Chinese Singaporeans. *European Spine Journal*, 13(2), 137–146.
25. Morgan, E. F., Bayraktar, H. H., & Keaveny, T. M. (2003). Trabecular bone modulus-density relationships depend on anatomic site. *Journal of Biomechanics*, 36(7), 897–904.
26. Yoganandan, N., Kumaresan, S., Voo, L., & Pintar, F. A. (1997). Finite element model of the human lower cervical spine: Parametric analysis of the C4–C6 unit. *Journal of Biomechanical Engineering*, 119(1), 87–92.
27. Guo, L. X., & Li, W. J. (2020). Finite element modeling and static/dynamic validation of thoracolumbar-pelvic segment. *Computer Methods in Biomechanics and Biomedical Engineering*, 23(2), 69–80.
28. Schileo, E., Taddei, F., Cristofolini, L., & Viceconti, M. (2019). Subject-specific finite element models implementing a maximum principal strain criterion are able to estimate failure risk and fracture location on human femurs tested in vitro. *Journal of Biomechanics*, 41(2008), 356–367.
29. Li, J., Huang, S., Tang, Y., Wang, X., & Pan, T. (2017). Biomechanical analysis of the posterior bony column of the lumbar spine. *Journal of orthopaedic surgery and research*. <https://doi.org/10.1186/s13018-017-0631-y>.
30. Kurutz, M., Donáth, J., Gálos, M., Varga, P., & Fornet, B. (2008). Age- and sex-related regional compressive strength characteristics of human lumbar vertebrae in osteoporosis. *Journal of Multidisciplinary Healthcare*, 1, 105–121.
31. Imai, K. (2015). Analysis of vertebral bone strength, fracture pattern, and fracture location: A validation study using a computed tomography-based nonlinear finite element analysis. *Aging and Disease*, 6(3), 180–187.
32. Røhl, L., Larsen, E., Linde, F., Odgaard, A., & Jørgensen, J. (1991). Tensile and compressive properties of cancellous bone. *Journal of Biomechanics*, 24(12), 1143–1149.
33. Iba, K., Wada, T., Takada, J., & Yamashita, T. (2003). Multiple insufficiency fractures with severe osteoporosis. *Journal of Orthopaedic Science*, 8(5), 717–720.
34. Cooper, C., Atkinson, E. J., Michael O'Fallon, W., & Melton, J. L. (1992). Incidence of clinically diagnosed vertebral fractures: A population-based study in rochester, minnesota, 1985–1989. *Journal of Bone and Mineral Research*, 7(2), 221–227.
35. Ismail, A. A., Cooper, C., Felsenberg, D., Varlow, J., Kanis, J. A., Silman, A. J., & Neill, T. W. O. (1999). International Original Article Number and Type of Vertebral Deformities : Epidemiological Characteristics and Relation to Back Pain and Height Loss. *Osteoporosis International*, 9, 206–213.
36. Bruno, A. G., Burkhart, K., Allaire, B., Anderson, D. E., & Bouxsein, M. L. (2017). Spinal Loading Patterns From Biomechanical Modeling Explain the High Incidence of Vertebral Fractures in the Thoracolumbar Region. *Journal of Bone and Mineral Research*, 32(6), 1282–1290.
37. Schmid, T., Heini, P., & Benneker, L. (2017). A rare case of non-traumatic, multi-level, bilateral pedicle fractures of the lumbar spine in a 60-year-old patient. *European Spine Journal*, 26, 1–5.
38. Seo, M. R. N., Park, S. Y., Park, J. S., Jin, W., & Ryu, K. N. (2011). Spinous process fractures in osteoporotic thoracolumbar vertebral fractures. *British Journal of Radiology*, 84(1007), 1046–1049.
39. Goel, V. K., Park, H., & Kong, W. (1994). Investigation of vibration characteristics of the ligamentous lumbar spine using the finite element approach. *Journal of Biomechanical Engineering*, 116(4), 377–383.